2010 IEEE International Conference on Robotics and Automation
Anchorage Convention District
May 3-8, 2010, Anchorage, Alaska, USA

A Two-Dimensional Passive Dynamic Running Biped with Knees

Dai Owaki, Masatoshi Koyama, Shin'ichi Yamaguchi, Shota Kubo and Akio Ishiguro

Abstract— **This is the first study of a real physical kneed bipedal robot that exhibits passive dynamic running (PDR). Passive dynamic walking (PDW), which has its roots in the pioneering research of McGeer, intrinsically offers not only nonlinear phenomena such as the *pull-in effect* and *period-doubling bifurcation*, but also offers an extremely interesting phenomenon that facilitates the engineering of a highly efficient walking robot. In recent years, a wide variety of verification experiments in PDW were performed using actual devices. In contrast, however, very few studies addressed PDR. In the present study, we developed a two-dimensional real physical passive dynamic running biped with knees. The device stands 400 mm tall and weights 4.8 kg. By carefully designing the properties of the elastic elements implemented into the hip joints and the stance legs in the present device, we achieved stable passive dynamic running of 36 steps. The device runs at about 0.83 m/s down a 0.22 rad slope. To the best of our knowledge, this is a first report of such a performance. This result is expected to prove useful not only for designing human-like natural and efficient bipedal robots, but also for understanding the principles underlying bipedal locomotion.**

I. INTRODUCTION

Living organisms possess an amazing ability to act and move adaptively within environments, which are non-structured and change unpredictably. We are interested in understanding the principles of the resilient and adaptive movement abilities of living organisms by designing a robot system that can behave adaptively, similar to what a living organism does. To that end, it is necessary to view a biological system as a control system, and then to understand the control laws of that control system. However, actual biological systems exhibit the "embedding problem" [1], in which a portion of the control laws are embedded within the object to be controlled. In other words, the behavior of biological systems are generated from the tight interaction between its control law (*i.e.* brain), the controlled object (*i.e.* body), and the environment [2], which makes it impossible to separate one from the other to discuss either of the entity separately.

This aspect of biological systems also strongly suggests that a certain amount of behavior-generation computation should be *offloaded* from the control laws to the object to be controlled (i.e. the mechanical structures and/or the material properties). To explicitly indicate this kind of "embodied" computation to be embedded in the controlled objects, Pfeifer *et al.* recently coined the term called "morphological computation" [3], [4], [5] which is expected to be an indispensable concept for building adaptive agents. Despite the appeal of this concept, there still remains a lot to be understood about how such "computational offloading" can be achieved to bring forth useful functionalities such as adaptivity. In this article, we refer to control laws embedded within controlled objects as "implicit control laws" and described algorithmic control laws as "explicit control laws". After the above considerations, it then becomes necessary to clarify the structure of implicit control laws, which should lead to an understanding of the embedding problem, which in turn should make sense of the mechanism behind the movement abilities of living organisms.

To understand the implicit control laws inherent within biological systems, it is essential to focus attention upon phenomena that strongly imply the existence of implicit control laws. Therefore, in the present study, we focused upon passive dynamic walking (PDW) [6] and passive dynamic running (PDR) [7]. There are collectively referred to as passive dynamic locomotion (PDL). PDL is generated purely from the interaction between the controlled object and environment. In these phenomena, robots possess no actuators or controllers whatsoever and continuously walk or run down slopes in a stable manner . In other words, PDL is a rare example of movement solely by means of implicit control laws, and such movement is also significant from a biological standpoint. Therefore, we expected to be able to understand the structure of implicit control laws during walking and running by focusing our attention on PDL.

Based on these considerations, Sugimoto and Osuka directed their attention to PDW [8] and drew an analytical Poincaré map for the ground contact points, thereby showing that the feedback structure inherent therein contributes to the stability of PDW. Conversely, Owaki et al. [9], like Osuka, et al., derived and analyzed a Poincaré map, but focused on PDR, thereby proving the inherent existence of a stabilization structure explained by a 2-Delay input control in accordance with dual input feedback [10]. Although our understanding of PDL continues to improve steadily thanks to these kinds of simulations and theoretical analyses, we feel that the three-prong approach of (i) simulations, (ii) theoretical analyses and (iii) experiments using actual devices is necessary to understand the phenomenon of PDL. From this standpoint, a wide variety of verification experiments [6], [11], [12] in PDW were performed using actual devices. However, although Sano et al., performed passive dynamic running experiments using actual devices [running experiments using spring-loaded rimless wheels [13] and running experiments using bars that focused upon erecting rotation movements [14]), until date no verification experiments using two-legged machines with knees were ever performed. Therefore, the

The authors are with Department of Electrical and Communication Engineering, Tohoku University, Sendai, Japan {owaki@cmplx./ishiguro@}ecei.tohoku.ac.jp

realization of passive dynamic bipedal running in an actual device would be an extremely significant accomplishment.

Therefore, the primary goal of this research is to realize passive dynamic bipedal running in an actual device. Our research is based upon findings, obtained through simulations [15] and theoretical analysis [9], and experimental verification was expected to yield new findings unobtainable from simulations, such as PDR in devices having legs with knees. For the present study, we constructed an actual passive dynamic bipedal running device and then performed running experiments, achieving a running performance of as many as 36 steps. We expect that these findings will contribute not only toward the design of a highly-efficient running robot, but also toward understanding the explicit principles of human running motion.

II. Design of 2D Passive Dynamic Running Biped

In this section, we present the actual device we constructed. We learned from the numerical simulations of [15] that two elastic parameters of a robot's body, namely the leg spring and the hip coil spring constants, play a pivotal role in generating various types of stable gait patterns, such as walking, running, skipping, etc. In light of these findings, we constructed for this research the two-dimensional passive dynamic running device with knees shown in Fig. 1. This two-dimensional model has four legs, two on the inside (inner legs) and two on the outside (outer legs), each of which move relative to the other. This method makes it possible to the restraint of movement in the roll and yaw directions, which we believed should allow for the easier realization of passive dynamic running as the first step toward a natural human-like running gait. The legs on the actual device were 400 mm long and 300 mm wide, with a mass of 4.8 kg. The specific characteristics of the actual device are:

(a) hip springs,
(b) leg springs,
(c) parallel-link mechanism,
(d) shock absorbers, and
(e) hyperextension mechanism.

These characteristics were developed through physical insight, experimentation, and lessons learned from previous passive dynamic walking devices [6], [11], [12], [16].

A. Hip Springs

Power is applied to the waist area close to the hip joint, and the device is equipped with a mechanism equivalent to a coil spring [referred to hereinafter as the hip spring, with a spring constant k_{hip} in Nm/rad, see Figs. 1 and 2 (a)]. This mechanism prevents the angle of the hip joint from opening too widely during the flight phase and also enables the regulation of the running cycle and running speed. Figure 3 (Extension 1) shows the mechanism developed in this study that is equivalent to a coil spring. As shown in this figure, plate-like parts with hinges (A) attached to the hip segment (B) are installed at upper anterior and posterior of inner and outer legs, respectively. These anterior and posterior plates are connected to one another by an elastic band (C) so

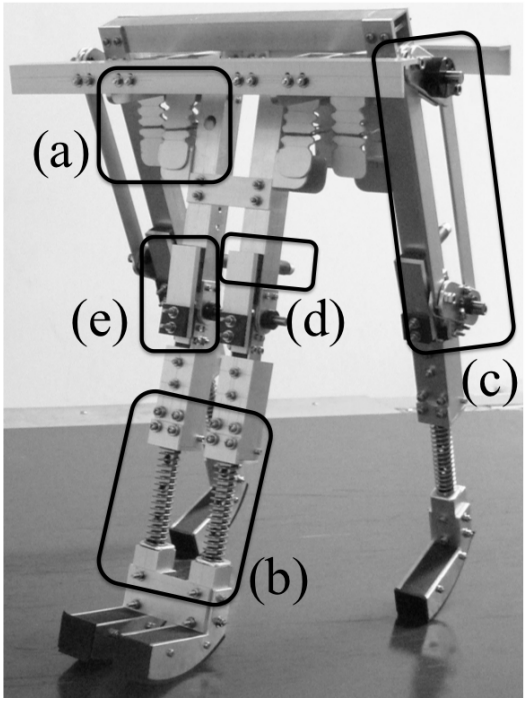

Fig. 1. Passive dynamic running biped (named *PDR400*). Height, width, and mass are 400 mm, 300 mm, and 4.8 kg, respectively.

that the angle between inner and outer legs cannot become too large. By carefully choosing the property of the elastic band, we can modify the parameter value k_{hip} in trial-and-error experiments. Through numerical simulation Van der Linde [17] and Kuo [18] showed that a passive walker with a compliant hip joint can change its walking velocity, and authors showed that hip spring becomes stiffer for the running gait than for walking gait in precious work [15]. Based on this knowledge, we can conclude the hip spring is the primary parameter for generating a running gait.

B. Leg Springs

The shank area is outfitted with a direct-action spring (referred to hereinafter as the leg spring, with a spring constant of k_{leg} in N/m), so energy is stored up when the leg spring contracts as the swing leg comes into contact with the ground, and this energy can be used for jumping [see Figs. 1 and 2 (b), and see also Extension 2]. By carefully choosing the property of the direct-action spring, we could modify the parameter value k_{leg} in trial-and-error experiments.

C. Parallel-Link Mechanism

To restrict movement across a flat, two-dimensional surface, both the inner legs must be synchronized and both the outer legs also must be synchronized. Although the inner legs are synchronized by contact between the femur area and the ankle area, the outer legs cannot be directly connected. Thus, to synchronize the movement of the outer legs, a parallel-link mechanism is used such that outer thigh and shank movement can be synchronized [see Figs. 1 and 2 (c)]. Figure 4 (Extension 3) shows the parallel-link mechanism illustrated

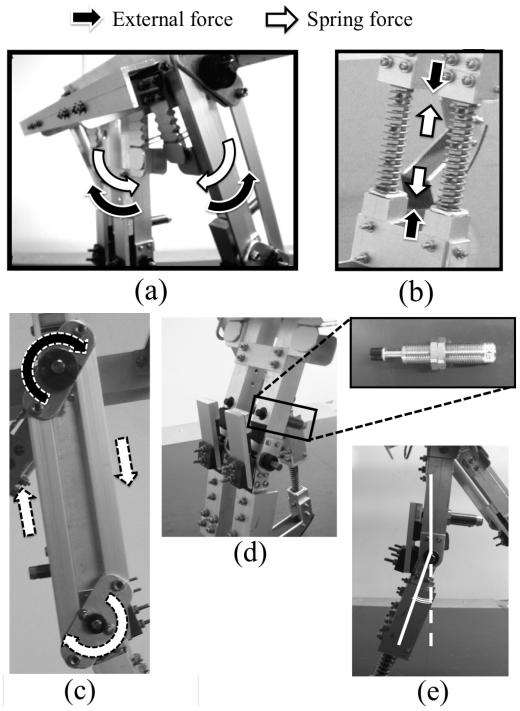

Fig. 2. Implementation of (a) torsion springs in the hip joints and (b) linear spring in the legs. Other key mechanisms are the parallel-link mechanism (c) shock absorbers (d) and hyperextension mechanism (e).

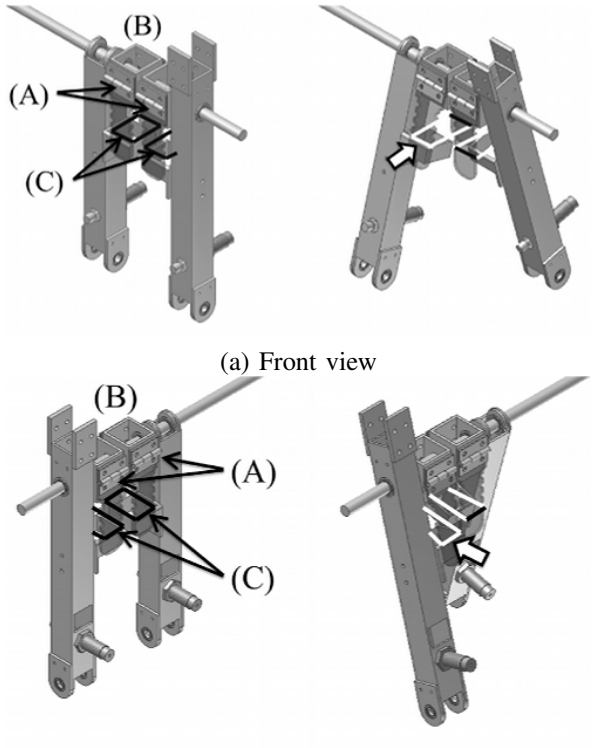

(a) Front view

(b) Back view

Fig. 3. Mechanism of hip spring that is equivalent to a coil spring (see also Extension 1).

by computer-aided design software and makes it apparent that the outer thigh segments (D) and (D') are synchronized by the direct connection bar (E) that is installed into the upper side in Fig. 4 (a). To synchronize the shank segments in the outer legs, we exploited this parallel-link mechanism shown in Fig. 4 (b) as follows: (i) A knee shaft rotates with movement of a shank segment; (ii) A rotating part attached to the knee shaft (F) rotates in sync with the knee rotation; (iii) A rotating part attached to the hip shaft (G) moves with this rotation through the parallel link; (iv) The other rotating part attached to the hip shaft (G') rotates in sync with the hip shaft rotation; and (v) Similar synchronization applies to the other shank segment. This mechanism allows the outer legs to synchronize properly. Note, however, that the leg springs have no synchronization mechanism to simplify the mechanical structures. We believe that this remaining problem does not significantly affect the results.

D. Shock Absorbers

In the areas of impact of the stoppers, the device is outfitted with shock absorbers that regulate the angle of the upper femur areas and the knee joints as shown in Figs. 1 and 2 (d). These shock absorbers prevent the curving of the knee joints that may otherwise be caused by impacts during knee joint extension or when the swing-leg makes contact with the ground.

E. Hyperextension Mechanism

The knee joints are outfitted with a hyperextension mechanism. Hyperextension is the condition wherein the knee joint bends through an excessively wide an angle such as shown in Fig. 2 (e). Equipping the device with a hyperextension mechanism improves the passive walking stability [16]. The angle of the hyperextension mechanism is θ in rad. Although humans do not exhibit hyperextension of the knee joint during running, our device needs this mechanism because it has no actuation. Our device cannot achieve running and without hyperextension it falls down because of bending knee joints without any actuations or elastic springs.

III. Experimental Results

A. Experimental Setting

Because of the limitations inherent in experiments involving rapid running movements on boards of a limited length, we performed running experiments using an inclined treadmill (MMW-H, Maruyasu Co., Inc., Sendai, Japan). The treadmill slope angle used in the experiment is denoted as α in rad. The adjustable parameters included the spring constant of the leg spring k_{leg}; the spring constant of the hip spring k_{hip}; the hyperextension angle θ; and the treadmill slope angle α. In addition, a high-speed camera (GE60W, Library Co., Inc., Tokyo, Japan) and a video measurement system (Move-tr/3D, Library Co., Inc., Tokyo, Japan) were also used for this experiment, allowing a detailed analysis of the movements of the running biped device.

B. Running Gait

To determine the experimental feasibility of passive dynamic running in the real world, we conducted running

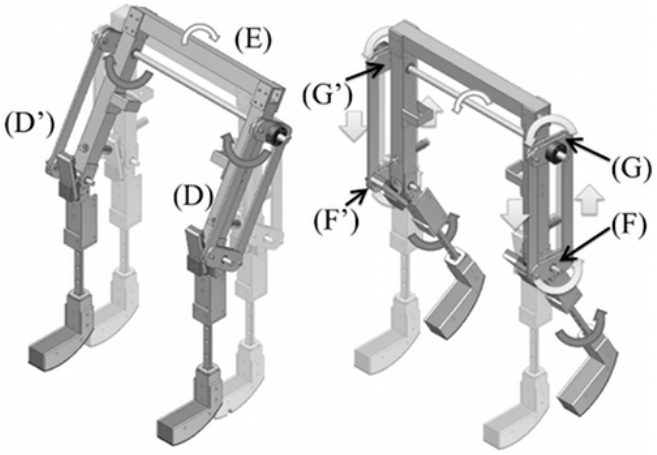

Fig. 4. Mechanism of parallel-link so that outer thigh and shank movement can be respectively synchronized (see also Extension 3).

experiments with various parameter settings (k_{hip}, k_{leg}, α, θ) and various initial conditions. In these experiments, we set the robot's parameters by trial-and-error through a vast number of trials. A maximum run of 36 steps was confirmed when the leg and hip springs are at $k_{leg} = 1200$ N/m and $k_{hip} = 0.6$ Nm/rad, respectively (see Extension 4 and 5). For this run, the slope angle was $\alpha = 0.22$ rad and the hyperextension angle was $\theta = 0.174$ rad, the running speed was $v = 0.833 \pm 0.020$ m/s and the Froude number was 0.42 by using $v/\sqrt{gl}$ [19]. We furthermore confirm a running cycle of $T_{run} = 0.417 \pm 0.010$ s, with $T_s = 0.350 \pm 0.025$ s during which the device was supported by only one leg, and $T_f = 0.067 \pm 0.025$ s during which none of the legs were in contact with the ground during each running cycle.

The running device is shown in Fig. 5, which displays a collection of photographs taken of the device throughout one running cycle across the sagittal plane. Note that in these photographs after a given leg has completed its stance period (i.e. the period during which it supports the device), it bounds forward (see image 7 in Fig. 5), then the device transits an flight period during which none of legs are in contact with the ground (see images 8 and 9 in Fig. 5) and then the swing-leg makes contact with the ground (image 10 in Fig. 5). Through a vast number of trials-and-errors, we found that the two elastic parameters k_{hip} and k_{leg} agree qualitatively with the simulation results. Thus, our experiment confirm that the hip and leg springs are the key parameters for generating gait patterns.

C. Quantitative Evaluation

Figure 6 (Extension 6) shows the motion trajectories of experimental PDR during three running cycles (in order from upper right to lower left). Figure 6 consists of stick diagrams for which position data from nine points (the toe-points of each leg, the arches of the feet, the heels, the knee joints, and the hip joint), measured by the video system, were plotted every 50 ms. The square within Fig. 6 shows the period during which none of legs are in contact with the ground,

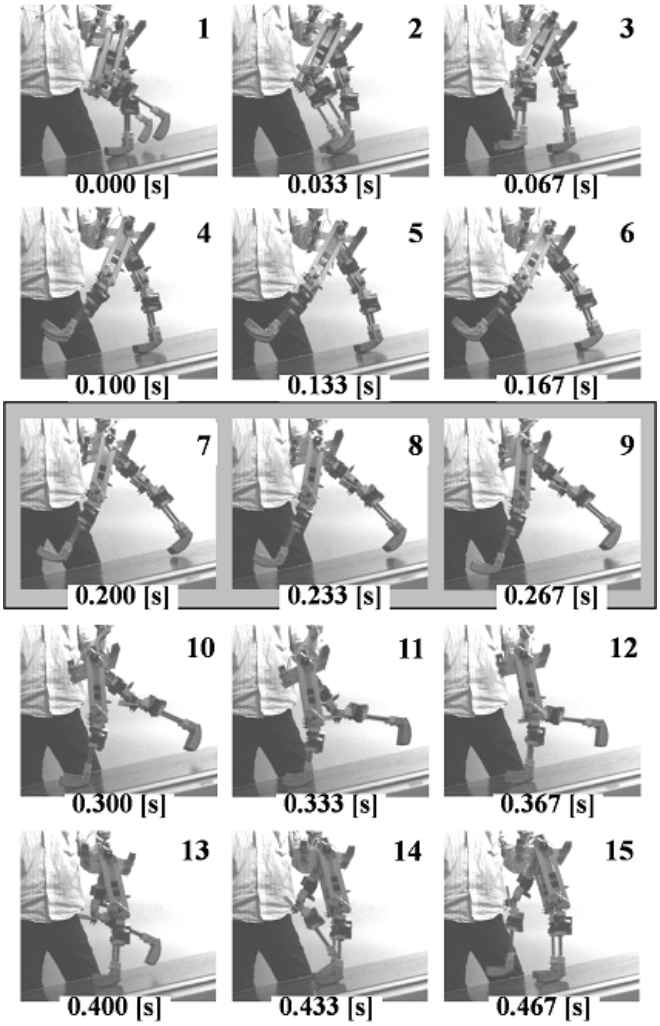

Fig. 5. Sequential photographs of a single running period. Note the flight period (0.067 s) during images 7–9 (see also Extension 4 and 5).

quantitatively confirming that, during this flight period none of legs are in contact with the ground, and that this occurs in each running cycle.

D. Robustness

To investigate the robustness as a function of initial conditions, we observed the rate of occurrence for each running-step range (e.g. 0–5, 6–10, 11–15, etc.) as a function of initial conditions. Figure 7 shows the success rate of passive dynamic running over 100 trials as a function of various initial conditions. This figure shows that our device can attain a running gait for more than 10 steps at a rate over 60% for various initial conditions. This result indicates that our device is robust against initial conditions because it exploits the elastic elements in its the hip joints and legs.

It is not easy to estimate the dimension of initial conditions and the stability in the experiment with a real robot in general. However, since we set these initial conditions by hand, the experiments validate the stability of running because we believe that the human element causes sufficient variations in initial conditions to test the stability of running versus initial

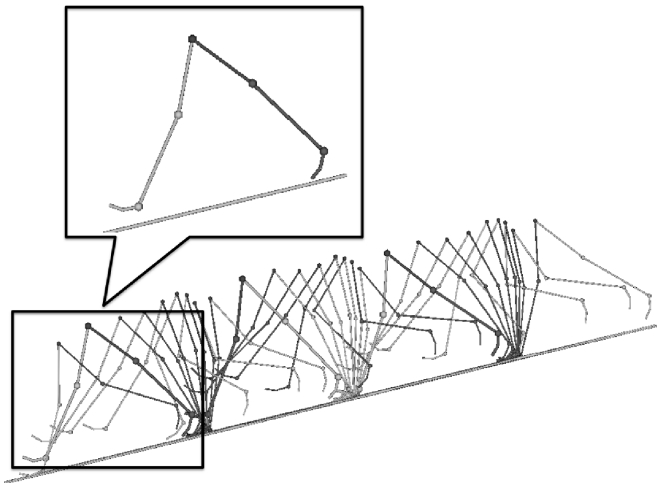

Fig. 6. Stick diagram of running motion during three periods, whose interval is 50 ms (see from right to left). We quantitatively confirmed that the flight period exists within each running cycle (see also Extension 6).

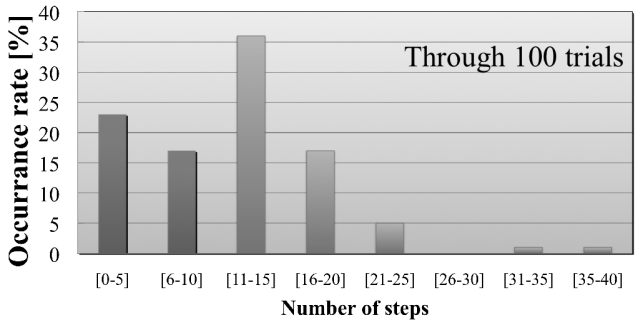

Fig. 7. Success rate over 100 trials of passive dynamic running for various initial conditions. Note that the running gait was observed at a rate over 60% for various conditions

conditions. The basin of attraction in the initial-condition space (which correlates with success rate for various initial conditions) explicitly correlates with the stability. In our previous work [9], we presented a theoretical analysis of the stability of the running gait and found the stabilization mechanism underlying passive dynamic running. Moreover, we found that the implicit two-delay feedback structure is an inherent stabilization mechanism as an implicit control law and this implicit control law strongly corroborates the self-stabilization mechanism of the running gait.

E. Ground Reaction Force

Figure 8 represents the time evolution of ground reaction force ($GRF_{\perp}$), which is perpendicular to the ground slope in PDR. These data are calculated by using the video measurement system, in which $GRFs_{\perp}$ are estimated by inserting the length of the shank segment l and the angle between the stance-leg and the ground slope θ_s into:

$$F_{GRF_{\perp}} = -k_{leg}(l - l_0)\sin(\theta_s),$$

where represents l_0 represents the rest length of the shank segment. Note that our device demonstrates a double-peak

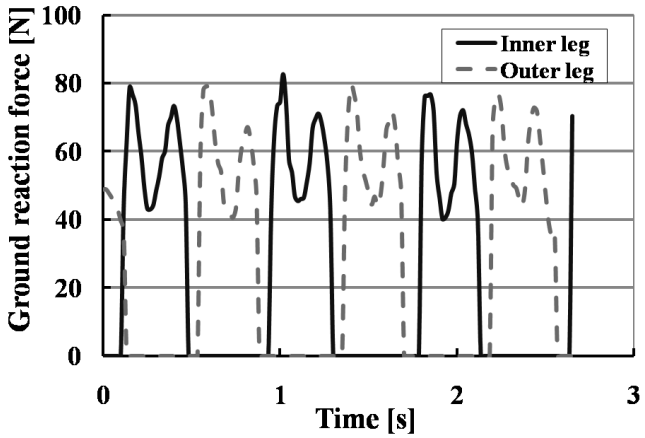

Fig. 8. Dynamics of ground reaction force perpendicular to the ground slope in passive dynamic running.

curve of $GFR_{\perp}$ during the stance period, which is different from the human-running profile [19]. However, we can see push-off from the ground slope just before landing, which has not been seen in previous PDW models [6], [12]. In future research, we will investigate the effect of these $GRF_{\perp}$ profiles on the stability of running, by demonstrating a single-peak curve of $GRF_{\perp}$ in PDR. Although there are many challenges yet to be solved, we believe that we have built the first real physical PDR device, which is the first step in the development of natural and efficient human-like running robots.

F. Discussion

The running gait of our PDR device is obviously not human-like in some respects. The motion of our bipedal running device includes a very short flight period and lift-off from the ground is insufficient. Moreover, the profile of $GRF_{\perp}$ shows a double-peak curve that is different from the human-running profile. Therefore, more work is necessary to directly explain human bipedal running. However, we cannot achieve human-like PDR that can explicitly explain human locomotion without the first studying actual two-dimensional PDR in the real world. We plan to address these remaining problems in the future to achieve natural and efficient human-like PDR.

IV. Conclusion

We presented an experimental verification of passive dynamic running (PDR). To this end, we developed a two-dimensional real physical PDR biped with knees. By carefully designing the properties of the elastic elements installed in the hip joints and the stance-leg, we achieved for the first time actual real-world PDR of 36 steps. Moreover, we confirm the existence of the flight period by measuring the motion trajectory of the running gait with a video measuring system. In addition, we investigated the robustness (i.e. the success rate) of PDR against various initial conditions, and observed the $GRF_{\perp}$ profile during the stance phase. These results suggest the feasibility of the implicit control laws

inherent within human-like running. We expect these results to prove useful not only for designing human-like natural and efficient bipedal robots, but also for understanding the principles underlying bipedal locomotion.

ACKNOWLEDGMENTS

This work was supported in part by a Grant-in-Aid for Young Scientists (Start-up) (21860007), for Scientific Research on Priority Areas "Emergence of Adaptive Motor Function through Interaction between Body, Brain and Environment", and by Tohoku Neuroscience Global COE Basic & Translational Research Center for Global Brain Science from the Japanese Ministry of Education, Culture, Sports, Science and Technology.

REFERENCES

[1] K. Osuka, A. Ishiguro, X. Zhen, Y. Sugimoto, and D. Owaki, "Implicit Control Law: A Common Principle of Mobiligence", *in Proc. of the 3rd International Symposium on Mobiligence in Awaji*, pp. 96–101, 2009.

[2] R. Pfeifer and C. Scheier, "Understanding Intelligence", *The MIT Press*, 1999.

[3] R. Pfeifer and F. Iida, "Morphological Computation: Connecting Body, Brain and Environment", *Japanese Scientific Monthly*, Vol.58, No.2, pp.48–54, 2005.

[4] C. Paul, "Morphological Computation", *in Proc. of the International Conference on Adaptive Behavior*, pp.33–38, 2004.

[5] K. Matsushita, M. Lungarella, C. Paul, and H. Yokoi, "Locomoting with Less Computation but More Morphology", *in Proc. of the 2005 IEEE International Conference on Robotics and Automation*, pp.2020–2025, 2005.

[6] T. McGeer, "Passive Dynamic Walking", *The International Journal of Robotics Research*, Vol. 9, No. 2, 1990, pp.62–82.

[7] T. McGeer, "Passive Dynamic Running", *in Proc. of the Royal Society of London, Series B, Biological Science*, Vol. 240, No. 1297, 1990, pp.107–134.

[8] Y. Sugimoto and K. Osuka, "Stability Analysis of Passive–Dynamic-Walking Focusing on The Inner Structure of Poincaré Map", *in Proc. of 12th International Conference on Advanced Robotics*, 2005.

[9] D. Owaki, K. Osuka and A. Ishiguro, "Understanding the Common Principle underlying Passive Dynamic Walking and Running", *in Proc. of The 2009 IEEE/RSJ International Conference on Intelligent Robots and Systems (IROS2009)*, pp. 3208–3213 2009.

[10] T. Mita, Y. Chida, Y. Kaku and H. Numasato, "Two-Delay Robust Digital Control and Its Applications –Avoiding the Problem on Unstable Limiting Zeros–", *IEEE Transactions on Automatic Control*, Vol. 35, No. 8, 1990, pp. 962–969.

[11] M. Coleman and A. Ruina, "An uncontrolled toy that can walk but cannot stand stillh, *Physical Review Letter*, Vol. 80, No. 16, pp. 3658–3661, 1998.

[12] S. H. Collins, M. Wisse, and A. Ruina, "A three-dimensional passive-dynamic walking robot with two legs and knees", *The International Journal of Robotics Research*, Vol. 20, No. 7, pp. 607–615, 2001.

[13] H. Miyamoto, Y. Ikemata, A. Sano, and H. Fujimoto, "Passive running of rimless wheel with springs", *in Proc. of CLAWAR'09*, pp. 269–276, 2009.

[14] A. Sano, S. Maruyama, Y. Ikemata, H. Miyamoto and H. Fujimoto, "A Study of Hinged-movement Aiming at Passive Running", *in Proc. of SI2008*, pp. 431–432, 2008 (*in Japanese*).

[15] D. Owaki , K. Osuka, and A. Ishiguro, "On the Embodiment that Enables Passive Dynamic Bipedal Running", *in Proc. of The 2008 IEEE International Conference on Robotics and Automation (ICRA2008)*, 2008, pp. 341–346.

[16] A. Ishiguro, M. Koyama, D. Owaki and J. Nishii, "Increasing Stability of Passive Dynamic Walking by Exploiting Hyperextension of Knee Joints", *in Proc. of 4th International Symposium on Adaptive Motion of Animals and Mechanics* (CD-ROM), 2008.

[17] R. Q. van der Linde, "Passive Bipedal Walking with Phasic Mulscle Contraction", *Biological Cybernetics*, Vol. 81, No. 3, pp. 227–237, 1999.

[18] A. D. Kuo, "Energetics of Actively Powered Locomotion using The Simples Walking Model", *Journal of Biomechanical Engineering*, Vol. 124, No.1, pp113–120, 2002.

[19] R. M. Alexander, *Walking and Running*, American Scientist, Vol. 72, pp.348–354, 1984.